



Title	NMR based serum extracts ' metabolomics for evaluation of canine Ehrlichiosis
Author(s)	Basoglu, Abdullah; Turgut, Kursad; Baspinar, Nuri; Tenori, Leonardo; Licari, Cristina; Ince, Mehmet Ege; Ertan, Merve; Suleymanoglu, Havva; Sayiner, Serkan
Citation	Japanese Journal of Veterinary Research, 68(4), 227-236
Issue Date	2020-11
DOI	10.14943/jjvr.68.4.227
Doc URL	<a href="http://hdl.handle.net/2115/79936">http://hdl.handle.net/2115/79936</a>
Type	article
File Information	JJVR68-4_227-236_AbdullahBasoglu.pdf



[Instructions for use](#)

## NMR based serum extracts' metabolomics for evaluation of canine Ehrlichiosis

Abdullah Basoglu<sup>1,\*</sup>, Kursad Turgut<sup>2)</sup>, Nuri Baspinar<sup>3)</sup>, Leonardo Tenori<sup>4)</sup>, Cristina Licari<sup>5)</sup>, Mehmet Ege Ince<sup>2)</sup>, Merve Ertan<sup>2)</sup>, Havva Suleymanoglu<sup>2)</sup> and Serkan Sayiner<sup>6)</sup>

<sup>1,\*</sup>) Department of Internal Medicine, Faculty of Veterinary Medicine, Selcuk University, Aleaddin Keykubat Campus, 42130 Selcuklu, Konya, Turkey

<sup>2)</sup> Department of Internal Medicine, Faculty of Veterinary Medicine, Near East University, Nicosia, TRNC

<sup>3)</sup> Department of Biochemistry, Faculty of Veterinary Medicine, Selcuk University, Aleaddin Keykubat Campus, 42130 Selcuklu, Konya, Turkey

<sup>4)</sup> Interuniversity Consortium for Magnetic Resonance of Metalloproteins (C.I.R.M.M.P.), Via Luigi Sacconi 6, 50019 Sesto Fiorentino (Florence), Italy

<sup>5)</sup> Magnetic Resonance Center (CERM), University of Florence, Via Luigi Sacconi 6, 50019 Sesto Fiorentino (FI), Italy

<sup>6)</sup> Department of Biochemistry, Faculty of Veterinary Medicine, Near East University, Nicosia, TRNC

Received for publication, May 20, 2020; accepted, August 16, 2020

### Abstract

Ehrlichiosis is an infection caused by obligate, intracellular organisms that primarily affect cells of the immune system in dogs, cats, and people. The objective of this study was to determine the changes in the plasma lipidome profiling of dogs with canine Ehrlichiosis and try to identify potentially useful metabolic markers. Our study animals included infected (92) and healthy (17) dogs. Indirect fluorescent-antibody assay (IFA) was used for the diagnosis of Ehrlichiosis. Anorexia, depression, hemorrhagic tendencies, enlarge lymph nodes are variable clinical signs of Ehrlichia. The hemogram reflected anemia and thrombocytopenia. There were no significant changes in other biochemical parameters. The individually identified metabolites seemed to be not effective in the characterization of the canine Ehrlichiosis. However, lipid fractions lead to the hypothesis that considerable differences among diseased and healthy animals could be found in their lipidome instead of the metabolome. This reflects a great systemic energy deficit during the infection.

Key Words: Ehrlichia, Metabolomics, NMR, Dogs

### Introduction

Ehrlichiosis is a tick-borne infection caused by obligate, intracellular organisms that primarily affect cells of the immune system in dogs, cats, and humans. In Europe published reports on this infection have increased in recent years. The prevalence of Ehrlichia infection in dogs is high and

different among European countries<sup>20)</sup>. In humans, Ehrlichia may cause hematologic malignancies, such as acute leukemia<sup>19)</sup>. The disease can evolve into a severe multisystem disease such as sepsis, meningoencephalitis or acute respiratory distress syndrome<sup>6)</sup>. An acute phase of disease, which develop during the subacute phase, starts in 2–4 weeks after exposure to *E.canis*. The chronic phase

\* Corresponding author: Abdullah Basoglu, e-mail: abbasoglu@selcuk.edu.tr, Department of Internal Medicine, Faculty of Veterinary Medicine, Selcuk University, Aleaddin Keykubat Campus, 42130 Selcuklu, Konya, Turkey  
Tel: +905063057744  
doi: 10.14943/jjvr.68.4.227

of the disease can develop in a few dogs. The main clinical symptoms of the disease are weakness, weight loss, and a tendency to bleed. If effective treatment is not applied, infected dogs are most likely to die<sup>7,17</sup>.

Diagnosis of canine Ehrlichiosis can be difficult to determine through blood smears, serology, and even PCR tests, this is because of their limitations to deal with the interpretation of test results according to the state of disease. IFA assay is still the diagnostic gold standard protocol for this disease<sup>4</sup>. A better understanding of the dynamics of canine Ehrlichiosis is necessary to reach the therapeutic targets. Metabolomics offers an objective approach to determine and understand the global metabolic pathways of infections. Variations in the metabolome reflect changes in the regulation of biochemical reactions, due to internal/external stimuli. Metabolite profiling can identify changes in host metabolism in response to infections. This will be the first NMR-based metabolomic study for canine Ehrlichiosis. The goal of this proposal is to obtain a metabolomics-level understanding of canine Ehrlichiosis.

## Material and Methods

The experimental design was approved by the Committee on Use of Animals in Research of the Near East University.

### Animals

The study animals included ninety-two infected and seventeen healthy dogs. The diseased dogs presented with some clinical signs which included a loss of appetite, depression, loss of stamina, stiffness and reluctance to walk, swelling of the limbs or scrotum, and coughing or difficulty in breathing.

### Laboratory analysis

Complete blood counts (leukocytes (WBC), erythrocytes (RBC), platelets (PLT), mean cell volume (MCV), mean corpuscular hemoglobin

concentration (MCHC), hematocrit (Ht), hemoglobin (Hb)), and biochemical profiles including total protein (TP), albumin (Alb), globulin, cholesterol, triglyceride, alanine amino transaminase (ALT), aspartate amino transaminase (AST), alkaline phosphatase (ALP), lactate dehydrogenase (LDH), blood urea nitrogen (BUN), creatinine and phosphorus were performed by routine automated cell counter and spectrometric methods, respectively. The infection in the animals was diagnosed by indirect fluorescent-antibody assay.

### Samples preparation for <sup>1</sup>H-NMR spectroscopy

Serum samples were thawed on ice and extracted for protein precipitation and separation of hydrophilic and lipophilic fractions with a dual methanol-chloroform extraction as described by Stringer et al.<sup>21</sup>. As a result of this, macromolecules (e.g., proteins) were eliminated and a fused metabolic profile for water-soluble and lipid metabolites was established.

A Bruker 600 MHz spectrometer (with a proton Larmor frequency of 600.13 MHz) was employed to acquire 1D NMR spectra for all analyzed samples. The instrument was assembled with a 2H-decoupling probe including a-z axis gradient coil, a 5 mm PATXI 1H-13C-15N, an automatic and refrigerated sample changer, and an automatic unit for tuning and matching (ATM). To avoid temperature variations (limited to  $\pm 0.1$ K at sample), a BTO 2000 thermocouple was used. Before initiating measurements, NMR tubes were maintained at 310K inside the NMR probe head for at least 5 minutes, to equilibrate temperature. A standard Nuclear Overhauser Effect Spectroscopy pulse sequence (noesygppr1d.com; Bruker BioSpin; NOESY 1D) was employed for both aqueous and organic serum extracts, as described in detail by Basoglu et al.<sup>1</sup>. For the aqueous fractions, a standard spin echo Carr-Purcell-Meiboom-Gill<sup>16</sup> pulse sequence (cpmgpr1d.com; Bruker BioSpin; CPMG) was also applied to acquire a second one-dimensional experiment using the same parameters described earlier<sup>1</sup>.

**Table 1.** Hematological and biochemical parameters between the animal groups.

	Diseased ( <i>n</i> =92)	Healthy ( <i>n</i> =17)	<i>P</i> value<0.05
WBCs (x10 <sup>3</sup> /μL)	9.9 (0.2/5390)	12.9 (7.70/38.2)	0,165
RBCs (x10 <sup>6</sup> /μL)	4.976±1.583	6.669±8.819	0,03
Platelets (x10 <sup>3</sup> /μL)	93 (0/1102)	277 (107/441)	0,001
Hgb (g/dL)	11 (2.2/18.6)	15.8 (6.2/18.2)	0,01
PCV (%)	33.436±11.643	48.318±10.087	0,01
Total protein (g/dL)	7.014±1.926	5.792±0.952	0,09
Albumin (g/dL)	2.058±0.575	2.8±0.372	0
BUN (mg/dL)	25.332±22.538	15.071±3.536	0,386
Urea (mg/dL)	22.69±1.590	47.525±9.326	0,159
Phosphorus (mg/dL)	4.06 (2.25/15.64)	4.4 (3.49/513)	0,781
Creatinine (mg/dL)	0.640 (0.18/3.86)	1.15 (0.44/1.15)	0,043
Triglyceride (mg/dL)	87.943 (41/115.940)	70.481 (8/21.405)	0,905
Cholesterol (mg/dL)	198.050±76.350	223.663±72.923	0,388
ALP (U/L)	115.35 (13.10/2461.65)	46.198 (12/277.04)	0,153
ALT (U/L)	61.385 (15/1472.24)	65.495 (39/100.17)	0,929
LDH (U/L)	212.791±151.811	142.828±100.768	0,124

WBC, PLT, ALP, ALT, BUN, phosphorus, creatinin, triglyceride = nonparametric (median (min/max)); RBC, Hgb, PCV, albumin, globulin, LDH, total protein, urea, cholesterol = parametric (mean±std).

### Spectral Processing

Before carrying out Fourier transform, free induction decays were multiplied by an exponential function equivalent to 0.3 Hz line-broadening factor. Obtained spectra were automatically corrected for phase and baseline distortions and calibrated using the software TopSpin 3.2 (Bruker BioSpin), considering as references, the anomeric glucose doublet signal at 5.24 ppm for serum aqueous extracts and the chloroform singlet at 7.24 ppm for the organic fractions.

One-dimensional spectra from aqueous extracts, in the range of 0.2-10.0 ppm, were divided into 0.02 ppm chemical shifts buckets and their corresponding spectral areas were integrated using AMIX software (version 3.8.4, Bruker BioSpin). Using the bucketing technique, the global number of variables is decreased and small shifts in the signals can be compensated allowing more reproducible and more robust analysis<sup>13</sup>.

Both regions between 4.62 and 4.75 ppm containing residual H<sub>2</sub>O signal and bins related to signals present only for a restricted number

of samples were excluded for the multivariate statistical analyses. Instead for organic fractions, only bins between 0.2 and 6.70 ppm were considered due to the presence of various shifts in the aromatic NMR signals of lipid molecules. On remaining bins, Probabilistic Quotient Normalization (PQN) was applied before performing the pattern recognition both for aqueous and organic extracts<sup>9</sup>.

### Statistical Analysis

In order to determine the normality for clinical and hematological parameters, the Kolmogorov-Smirnov test was used, while for comparison between groups, the Mann-Whitney U test was performed for non-parametric cases and the Independent-T test was used for parametric ones.

All metabolomic analysis were done using R, an open source software for statistical manipulation of data<sup>14</sup>. Multivariate analysis was applied on processed NMR data and to preliminarily explore the dataset, Principal Component Analysis (PCA) technique was employed<sup>22</sup>.

When unsupervised approach was not able to

**Table 2.** Concentrations in arbitrary units (median  $\pm$  Median Absolute Deviation (MAD)) of metabolites and lipid fractions assigned in serum samples (both aqueous and organic extracts). Statistically significant adjusted  $P$  value  $< 0.05$  are also reported.

	Metabolites	Diseased ( $n=92$ ) (arbitrary units)	Healthy ( $n=17$ ) (arbitrary units)	$P$ value
<b>Serum aqueous fraction (SWS)</b>	3-hydroxybutyrate	0.02 $\pm$ 0.01	0.02 $\pm$ 0.00	
	3-hydroxyisobutyrate	0.01 $\pm$ 0.002	0.01 $\pm$ 0.002	
	Acetate	0.385 $\pm$ 0.065	0.37 $\pm$ 0.08	
	Alanine	0.1 $\pm$ 0.03	0.12 $\pm$ 0.03	
	Citrate	0.07 $\pm$ 0.02	0.08 $\pm$ 0.02	
	Choline	0.01 $\pm$ 0.00	0.02 $\pm$ 0.01	
	Creatine	0.01 $\pm$ 0.005	0.007 $\pm$ 0.002	
	Creatinine	0.03 $\pm$ 0.01	0.04 $\pm$ 0.01	
	formate	0.07 $\pm$ 0.01	0.06 $\pm$ 0.01	
	Glycine	0.04 $\pm$ 0.01	0.06 $\pm$ 0.015	
	D-Glucose	0.18 $\pm$ 0.06	0.17 $\pm$ 0.065	
	Isoleucine	0.02 $\pm$ 0.01	0.02 $\pm$ 0.005	
	Lactate	1.015 $\pm$ 0.22	1.08 $\pm$ 0.255	
	Leucine	0.05 $\pm$ 0.02	0.05 $\pm$ 0.01	
	Phenylalanine	0.03 $\pm$ 0.02	0.04 $\pm$ 0.015	
	Pyruvate	0.06 $\pm$ 0.01	0.08 $\pm$ 0.02	
Tyrosine	0.02 $\pm$ 0.01	0.02 $\pm$ 0.01		
Valine	0.06 $\pm$ 0.02	0.07 $\pm$ 0.02		
<b>Serum organic fraction (SLS)</b>	Cholesterol C(18)H <sub>3</sub>	0.011 $\pm$ 0.0033	0.0135 $\pm$ 0.002	
	Cholesteryl ester	0.0016 $\pm$ 0.0005	0.048 $\pm$ 0.008	
	Fatty acid -CH=CH-CH <sub>2</sub> -CH=CH-	0.0065 $\pm$ 0.002	0.011 $\pm$ 0.0032	<0.05 (diseased versus healthy)
	Fatty acid -(CH <sub>2</sub> ) <sub>n</sub> -	0.19 $\pm$ 0.05	0.245 $\pm$ 0.02	
	Fatty acid -CH <sub>3</sub>	0.017 $\pm$ 0.005	0.022 $\pm$ 0.005	
	Fatty acid -CH <sub>2</sub> -CO	0.0052 $\pm$ 0.0015	0.00735 $\pm$ 0.0012	<0.05 (diseased versus healthy)
	Fatty acid =CH-CH <sub>2</sub> -CH <sub>2</sub>	0.016 $\pm$ 0.005	0.02 $\pm$ 0.002	
	Glycerol backbone	0.00051 $\pm$ 0.00017	0.00027 $\pm$ 0.000225	<0.05 (diseased versus healthy)
Polyunsaturated fatty acids (18:2, bis allylic protons)	0.0066 $\pm$ 0.0018	0.008 $\pm$ 0.0016		
Unsaturated fatty acid -CH=CH-	0.034 $\pm$ 0.009	0.048 $\pm$ 0.008	<0.05 (diseased versus healthy)	

discriminate between the conditions of interest, Orthogonal Projection to Latest Structures (OPLS) analysis is applied in combination with Discriminant Analysis (DA) as a supervised method. In general, this algorithm uses information in the categorical response  $Y$  matrix to separate, in the  $X$  matrix of data, the predictive from non-predictive ( $Y$ -orthogonal) variation, providing a better model interpretation with respect to PCA or to the PLS techniques<sup>23)</sup>.

All the accuracies and confusion matrices

reported for the various classifications were assessed by means of 100 cycles of Monte Carlo cross-validation scheme (MCCV, R script in-house written). Further explanations have been reported earlier<sup>1)</sup>.

Univariate statistical analysis was performed on <sup>1</sup>H-NMR spectra. In particular, well defined and resolved spectral regions associated to the different metabolites/lipid fractions were assigned by using matching routines of Assure NMR (Bruker BioSpin) and published literature data. The same

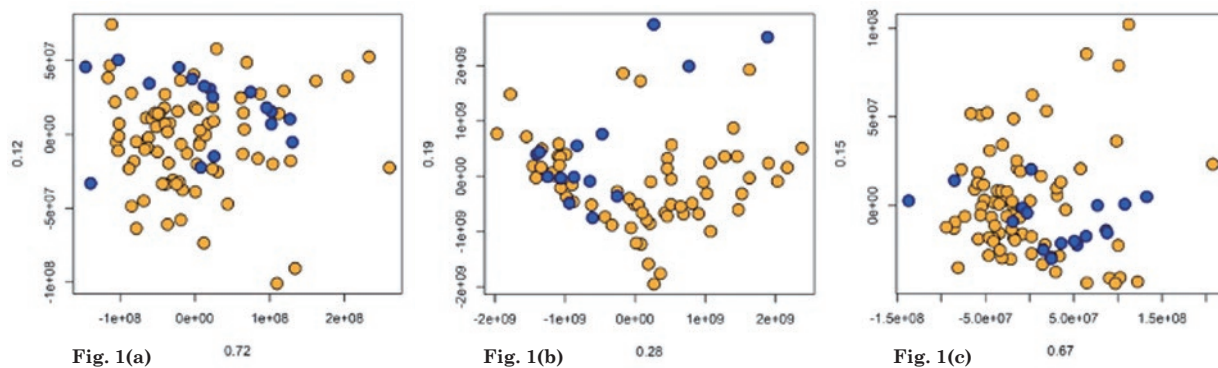


**Fig. 1 (a – c).**

Principal component analysis (PCA) score plots. Each dot represents a single  $^1\text{H-NMR}$  spectrum. Diseased animals ( $n=92$ ) are represented in orange, while the healthy ( $n=17$ ) in blue. The variance related to the first principal component (PC1) is reported in the X-axis, while the variance related to the second principal component is reported in the Y-axis. **a** PCA on 1D NOESY spectra of serum aqueous fractions; **b** PCA on 1D NOESY spectra of serum organic fractions; **c** PCA on 1D CPMG spectra of serum aqueous extracts.

regions were integrated to obtain concentrations of metabolites and lipidic fractions in arbitrary units.

Resulting values were analyzed to find discriminating metabolites between the diseased and healthy dogs using a non-parametric Wilcoxon-Mann-Whitney test on the biological assumption that metabolites and lipids concentrations are not normally distributed<sup>18)</sup>.

When several metabolites/lipids are tested together, to avoid random false positives, multiple testing corrections need to be adopted; here, the Benjamini-Hochberg method (FDR) was applied<sup>5)</sup>.

Then, changes in metabolites/lipids levels between the two compared groups are calculated as the log<sub>2</sub> fold change (FC) ratio of the normalized median intensities of the corresponding signals in the spectra.

Commonly, to express correlation among different metabolites expression levels and clinical and/or other biological data, correlation coefficients must be calculated.

Spearman's test was used to express the correlation coefficients ( $\rho$ ) among the metabolite concentrations of diseased animals and the clinical features. Values between +1 and -1 are reported, where +1 indicates a total positive correlation, 0 means no correlation, and -1 is related to a total negative correlation. All correlation coefficients were calculated using the "cor. test" function of R

software. Graphical representations of correlation matrices of metabolites and lipid fractions were displayed using the R "corrplot" package.

## Results

Anorexia, depression, hemorrhagic tendencies, large lymph nodes were variable clinical symptoms of Ehrlichia. The hemogram reflected anemia and thrombocytopenia. There were no significant changes in biochemical parameters (Table 1). Serum indirect fluorescent antibody titers were positive in all the diseased animals.

One-dimensional  $^1\text{H-NMR}$  spectra of serum samples were acquired. Eleven diseased animals were not considered for the statistical analysis of serum aqueous extracts because of the inadequate quality of the related NMR spectra, while a total of thirty-two dogs were removed from the analysis of organic fractions for same reasons.

Diseased animals were compared with healthy ones using a first unsupervised approach, in the PCA. No apparent differences or clusters were highlighted among the groups, but from the analysis of 1D NOESY and 1D CPMG spectra of aqueous extracts, one and three subjects were respectively identified as evident outliers and therefore eliminated for the subsequent analyses.

**Table 3.** Spearman's rho correlation coefficients between metabolites/lipids concentrations and measured blood parameters of diseased animals. Positive correlation coefficient values higher than 0.60 are in light gray, while negative rho coefficients smaller than 0.60 are in dark gray.

	WBC	RBC	HGB	HCT	PLT	Albumine	Globulin	ALP	ALT	BUN	P	Creatinine	LDH	Total Protein	Triglycerides	Cholesterol
Alanine	0.06	0.14	0.18	0.18	0.07	0.04	-0.17	0.19	0.28	0.10	0.04	-0.01	0.38	-0.15	0.29	-0.07
Valine	0.01	0.01	0.03	0.04	0.14	0.02	-0.10	0.03	0.14	0.33	0.21	0.03	0.25	0.00	0.22	-0.05
Leucine	0.02	0.09	0.08	0.09	0.09	0.12	-0.25	0.05	0.19	0.15	0.12	-0.07	0.22	-0.10	0.16	0.00
L-Isoleucine	0.02	-0.07	-0.06	-0.05	-0.03	0.11	-0.18	0.15	0.08	0.16	0.11	-0.10	0.22	-0.10	0.11	0.08
Lactate	0.26	-0.08	-0.05	-0.05	-0.07	-0.23	0.14	0.30	0.19	0.14	0.07	0.02	0.30	0.08	0.29	0.06
Acetate	0.17	0.05	0.05	0.02	0.14	-0.02	-0.25	0.17	0.53	-0.10	0.11	-0.03	0.29	-0.24	0.04	0.12
Citrate	0.09	0.09	0.18	0.12	0.48	-0.07	0.09	-0.09	0.18	0.11	0.18	0.17	-0.07	0.11	-0.03	0.06
Creatinine	0.31	0.11	0.18	0.16	0.14	-0.07	-0.06	-0.34	-0.03	0.20	0.23	0.58	0.03	-0.08	0.13	0.28
Creatine	0.30	0.09	0.09	0.08	0.03	0.12	-0.42	-0.03	-0.17	0.25	0.06	0.20	0.16	-0.35	0.20	0.34
L-Pyroglutamate	-0.06	0.03	0.08	0.07	0.07	0.19	-0.14	-0.17	0.16	-0.29	-0.07	-0.15	0.07	-0.11	-0.14	-0.17
D-Glucose	0.12	-0.25	-0.34	-0.32	-0.13	-0.35	0.04	0.05	0.07	-0.18	0.06	-0.28	0.21	-0.12	-0.08	-0.10
3-Hydroxybutyrate	-0.10	-0.24	-0.17	-0.20	0.27	-0.12	0.04	-0.10	0.18	0.20	0.27	0.01	-0.12	0.06	0.10	0.02
Choline	0.18	0.06	0.03	0.05	0.17	0.09	-0.33	-0.06	-0.02	0.24	0.15	0.15	0.28	-0.31	0.21	0.13
Glycine	0.12	-0.05	-0.05	-0.07	-0.19	0.07	-0.19	0.26	0.05	-0.11	-0.12	0.02	0.24	-0.25	0.31	0.24
Tyrosine	-0.05	0.28	0.30	0.27	0.01	0.05	-0.12	0.34	0.60	0.05	-0.09	0.03	0.25	-0.12	-0.01	0.15
Phenylalanine	0.11	0.03	0.01	0.00	-0.11	-0.02	-0.22	0.24	0.39	0.02	-0.03	0.06	0.35	-0.24	0.28	0.42
Xanthine	-0.11	-0.36	-0.37	-0.39	-0.27	-0.23	-0.08	0.12	0.32	0.07	0.24	0.07	0.26	-0.24	0.17	-0.05
Formate	0.11	-0.01	-0.02	-0.06	0.15	-0.08	-0.11	0.14	0.26	0.03	0.07	-0.19	0.27	-0.10	0.08	-0.03
Pyruvate	0.06	0.30	0.31	0.31	0.19	0.35	-0.23	-0.07	0.01	-0.45	-0.18	-0.35	0.13	-0.17	-0.13	-0.04
3-Hydroxyisobutyrate	0.13	-0.45	-0.42	-0.45	0.02	-0.34	0.19	0.12	0.17	0.44	0.31	0.20	0.12	0.28	0.25	-0.10
Isobutyrate	-0.06	0.07	0.10	0.07	-0.08	0.06	-0.11	0.03	0.19	-0.12	-0.05	-0.18	-0.01	-0.04	0.06	-0.17
Fas-CH <sub>3</sub>	0.25	0.17	0.15	0.18	0.12	0.53	-0.61	-0.14	-0.22	0.16	-0.02	0.18	0.04	-0.56	0.16	0.70
Fas-(CH <sub>2</sub> ) <sub>n</sub>	0.20	0.14	0.10	0.14	0.07	0.58	-0.66	-0.13	-0.27	0.15	-0.05	0.06	0.13	-0.59	0.24	0.59
Fas=CH-CH <sub>2</sub> -CH <sub>2</sub>	0.22	0.22	0.19	0.22	0.13	0.66	-0.71	-0.14	-0.23	0.14	-0.10	0.06	0.11	-0.59	0.21	0.60
Fas-CH <sub>2</sub> -CO	0.22	0.26	0.23	0.25	0.21	0.58	-0.64	-0.15	-0.22	0.08	-0.03	0.12	0.05	-0.59	0.18	0.71
PUFA	0.26	0.18	0.16	0.18	0.14	0.65	-0.69	-0.15	-0.22	0.15	-0.10	0.07	0.14	-0.57	0.24	0.61
Fas-CH=CH-CH <sub>2</sub> -CH=CH	0.04	0.39	0.35	0.39	0.08	0.46	-0.69	-0.04	-0.06	0.19	0.05	0.12	0.08	-0.59	0.04	0.55
Phosplip-N(CH <sub>3</sub> ) <sub>3</sub>	0.17	0.24	0.21	0.25	0.08	0.58	-0.70	-0.13	-0.16	0.12	-0.01	0.11	0.14	-0.62	0.13	0.62
Glycerol	0.11	-0.11	-0.17	-0.13	0.01	0.31	-0.48	-0.03	-0.02	0.43	0.13	0.01	0.22	-0.39	0.68	0.25
Cholesteryl ester	0.25	0.22	0.22	0.24	0.16	0.54	-0.57	-0.14	-0.22	0.13	-0.06	0.16	0.01	-0.52	0.14	0.69
UFA-CH=CH	0.18	0.28	0.24	0.27	0.11	0.62	-0.72	-0.08	-0.18	0.12	-0.08	0.07	0.13	-0.61	0.20	0.64
Cholesterol(C18)H <sub>3</sub>	0.27	0.15	0.13	0.16	0.11	0.49	-0.61	-0.16	-0.17	0.19	0.01	0.22	0.07	-0.57	0.18	0.70

PCA score plots on 1D NOESY and 1D CPMG of serum aqueous fractions and on 1D NOESY of serum organic extracts are reported in Fig. 1 (a-c).

To explore differences in the metabolic profile of diseased and healthy animals, a Monte Carlo cross-validated OPLS-DA model was built for both aqueous and organic extracts, randomly sampling among diseased group a comparable number of

samples to the healthy group. Models built on 1D NOESY and 1D CPMG spectra of aqueous fractions provide average accuracies of 68% and 72% respectively, suggesting the presence of slight metabolic differences between healthy and diseased animals. Instead, an average discrimination accuracy of 76% between the two groups of subjects was defined considering the 1D NOESY spectra of



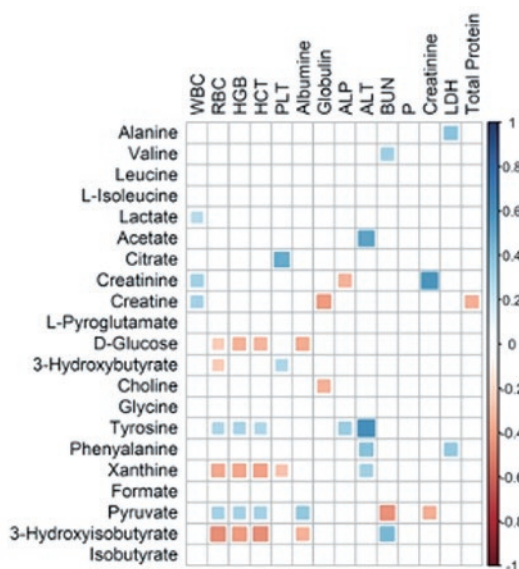


Fig. 2(a)

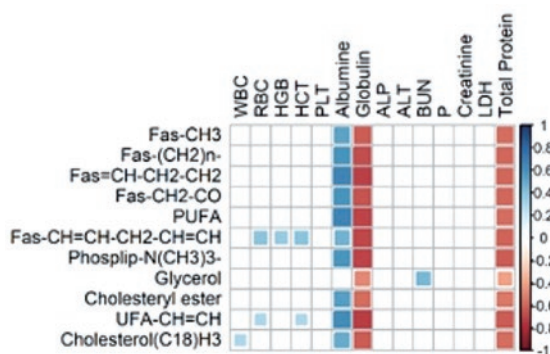


Fig. 2(b)

Fig. 2 (a – b).

Graphical representations of correlation matrices between metabolites (a), lipid fractions (b), (reported in the rows) and blood parameters (reported in columns). Only glyphs that are representatives for a statistically significant correlation ( $P$  values  $<0.05$ ) are reported and colored following a gradient that ranges from dark red to dark blue according to Spearman's rho correlation coefficients from -1 to +1.

organic fractions, leading to the hypothesis that the considered diseases affects more the lipidome of the dogs (Table 2).

In order to identify the presence of discriminating metabolites among the two groups of interest,  $^1\text{H-NMR}$  spectra were also examined. The complete list of identified and quantified metabolites from each type of sample (lipophilic and hydrophilic fractions) is presented in Table 2, where adjusted  $P$  values are reported only for variables that differ significantly (adjusted

$P$  value  $<0.05$ ) after performing the comparison using the Wilcoxon-Mann-Whitney test. Among the eighteen identified metabolites, none of them resulted in being statistically different between diseased and healthy dogs (all adjusted  $P$  values  $>0.05$ ). From the univariate analysis of serum lipids, the results showed that signals of alkyl chains of fatty acids arising from unsaturated fatty acid protons  $-\text{CH}=\text{CH}$  and  $-\text{CH}_2-\text{CO}$ ,  $-\text{CH}=\text{CH}-\text{CH}_2-\text{CH}-\text{CH}$  protons were higher and statistically different (adjusted  $P$  values  $<0.05$ ) for healthy animals, while glycerol resulted in being significantly higher for the diseased dogs (adjusted  $P$  value  $<0.05$ ). These last results are in line with the fact that OPLS-DA model built on 1D NOESY of organic fractions showed a higher predictive accuracy than that one reported for aqueous extracts.

In summary, the obtained results demonstrate that we can define a likely fingerprint of the disease considering the whole metabolic profile of animals (NMR spectra in their entirety), since the individually identified metabolites seem to be not effective in the characterization of the canine Ehrlichiosis. However, the existence of four statistically significant lipid fractions lead to the hypothesis that considerable differences among diseased and healthy animals could be found in their lipidome instead of the metabolome (Table 2). Correlations among identified metabolites/lipid fractions and clinical data were expressed for the diseased animals.

Spearman's test was used to calculate the correlation coefficients (rho) between metabolomic data and blood parameters. In particular, it was found that albumin positively correlate with proton signals of alkyl chains from fatty acids arising from  $=\text{CH}-\text{CH}_2-\text{CH}_2$ ,  $\text{UF}=\text{CH}-\text{CH}$  groups and from PUFA (rho coefficient higher than 0.60), while tyrosine positively correlates with ALT values (rho coefficient equal to 0.60). Instead, globulins negatively correlate with all the identified lipid fractions except for glycerol and cholesteryl ester fractions (rho values less than -0.60). Negative correlations were also identified for total proteins values with phospholipids- $\text{N}(\text{CH}_3)_3$  and unsaturated



-CH=CH- protons. All calculated correlation coefficients ( $\rho$ ) are reported in Table 3.

Graphical representations of correlation matrices of metabolites and lipid fractions are reported in Fig. 2 (a-b) where only statistically significant correlations ( $P$  values  $<0.05$ ) are highlighted and represented through glyphs that are coloured according to the calculated  $\rho$  coefficients and whose respective values (from -1 to +1) are shown on the gradient coloured-bar located in the right-side of the figures.

## Discussion

This is the pioneer metabolomic and lipidomic study carried out on dogs suffering from ehrlichiosis. Identified lipidome profiling in this study will give an opportunity for further mechanistic studies to better understand the host responses in Ehrlichia infection.

Ehrlichiosis is a bacterial illness that affects humans and animals causing flu-like symptoms. Many individuals have mild symptoms and never seek medical attention. However, life-threatening cases of Ehrlichiosis manifest as meningoencephalitis or acute respiratory distress syndrome together with sepsis<sup>6</sup>. Ehrlichia can also lead to hematologic malignancies<sup>19</sup>. Most often, a diagnosis is performed by a combination of clinical signs, positive serum IFA titer and response to treatment<sup>8</sup>. In the current study, either clinical signs or hematological parameters of seropositive dogs were in accordance with most references (Table 1).

Metabolites with extraordinary array of physicochemical properties, produced by microbial and host cells, may be found in any body tissue or fluid at varying concentrations. Determination of omics produced from the host-response to bacterial infection seems to be very useful. Metabolomics has a great potential to determine new biomarkers of diseases, useful to identify for example, early stage diseases, thus potentially addressing an important clinical need. Performing new studies on

metabolomics, low-cost biomarkers from body fluids that indicate infection, therapeutic efficacy, or drug resistance might be identified. In particular, with advantages of minimal sample preparation, high throughput, high reproducibility and high accuracy, metabolomic analyses provide great potentialities for diseases diagnosis and treatment with respect to classical clinic tests. Moreover, with respect to traditional techniques used to explore biomarker profiles, metabolomics offers complete information on low- and high-molecular-weight metabolites present in biofluids. Therefore, metabolomics gives the possibility to generate innovative and non-invasive diagnostic tests providing a unique insight into already known and novel metabolic pathways, which are simple and cost-effective yet retaining high sensitivity and specificity properties<sup>24</sup>. Despite the impact of metabolomics on infectious diseases, no study has been done in regards to Ehrlichiosis infections<sup>10,11</sup>.

Lipids have important roles in various cellular processes. Changes in the lipidome, in addition of nucleic acid and proteins, can be evaluated as biomarkers. The role of lipids in especially bacterial infections are well recognized by the human innate immune response, such as lipopolysaccharide in Gram-negative bacteria, lipoteichoic acid in Gram-positive bacteria, and lipoglycans in mycobacteria. When we compared nucleic acids and protein analysis, a complete analysis of the lipidome is usually very difficult due to the heterogeneity of lipid classes and their intrinsic physical properties caused by variations in the constituents of each class. Therefore, their biological relevance and their use as potential biomarkers for non-infectious and infectious diseases is crucial. Sepsis and tuberculosis are the two primary diseases in which lipids can be diagnosed using biomarkers<sup>15</sup>. In septic patients, lipid profiles may be a predictor of survival. In metabolomic studies, most of the changes from baseline in septic patients are related to lipid metabolism<sup>12</sup>.

NMR-based metabolomics has been evaluated in diarrheic and presumed septic calves, where significant decreases in the whole lipid soluble

metabolites such as sphingomyelin and fatty acids including PUFA were found. Other characteristic metabolites, such as increases in niacinamide, choline + phosphocholine, 2-methylglutarate and isopropanol, and decreases in format, lysine-arginine, acetate, creatine also reflected the systemic inflammatory response syndrome, organ dysfunction and organ failure<sup>3)</sup>. NMR metabolomics provided an optimal tool for faster identification of sepsis in newborn calves<sup>2)</sup>. In the present study, among the eighteen metabolites which were identified, none of them resulted to be statistically different between diseased and healthy dogs (Table 2). Ehrlichiosis affected more the lipidome of the dogs. Alkyl chains of fatty acids arising from UFA-CH=CH, -CH<sub>2</sub>-CO, -CH=CH-CH<sub>2</sub>-CH-CH protons were higher and statistically different for healthy, while glycerol resulted in being significantly higher in the diseased animals. Decrease in the whole lipid soluble metabolites mentioned above may indicate a great systemic energy deficit in canine Ehrlichiosis. The correlations of lipid metabolites with blood proteins may be meaningful in this regard (Table 3).

### Acknowledgments

CERM/CIRMMP center of the ESFRI Instruct is gratefully acknowledged for the NMR access provision financially supported by the EC Contract iNEXT No 653706.

### References

- 1) Basoglu A, Baspinar N, Tenori L, Licari C, Gulersoy E. Nuclear magnetic resonance (NMR)-based metabolome profile evaluation in dairy cows with and without displaced abomasum. *Veterinary Quarterly* 40, 1-15, 2020.
- 2) Basoglu A, Sen I, Meoni G, Tenori L, Naseri A. NMR based plasma metabolomics at set intervals in newborn dairy calves with severe sepsis. *Mediators of Inflammation* 2018; doi:10.1155/2018/8016510, 2018.
- 3) Basoglu A, Baspinar N, Tenori L, Hu X, Yildiz R. NMR based metabolomics evaluation in neonatal calves with acute diarrhea and suspected sepsis: a new approach for biomarker/s, *Metabolomics Open acces* 2, 134, 2014.
- 4) Bélanger M, Heather L. Sorenson HL, France MK, Bowie MV, Barbet AF, et al. Comparison of serological detection methods for diagnosis of Ehrlichia canis infections in dogs. *Journal of Clinical Microbiology* 40, 3506–3508, 2002.
- 5) Benjamini Y and Hochberg Y. Controlling the false discovery rate: a practical and powerful approach to multiple testing. *J R Stat Soc Ser B Methodol* 289–300, 1995.
- 6) Buzzard SL, Bissell BD, Melissa L. Bastin T. Ehrlichiosis presenting as severe sepsis and meningoencephalitis in an immunocompetent adult. *JMM Case Rep.* 5, e005162, 2018.
- 7) Chochlios TA, Angelidou E, Kritsepi-Konstantinou M, Koutinas CK, Mylonakis ME. Seroprevalence and risk factors associated with Ehrlichia canis in a hospital canine population. *Vet Clin Pathol* 48, 305–309, 2019.
- 8) Csokai J, Klas EM, Heusinger A, Müller E. Occurrence of Ehrlichia canis in dogs living in Germany and comparison of direct and indirect diagnostic methods. *Tierarztl Prax Ausg K Kleintiere Heimtiere* 45, 301-307, 2017.
- 9) Dieterle F, Ross A, Schlotterbeck G, Senn H. Probabilistic quotient normalization as robust method to account for dilution of complex biological mixtures. Application in 1H NMR metabonomics. *Anal Chem* 78, 4281–90, 2006.
- 10) Eoh H. Metabolomics: a window into the adaptive physiology of Mycobacterium tuberculosis. *Tuberculosis* 94, 538–543, 2014.
- 11) Fuchs TM, Eisenreich, W, Heesemann J, Goebel W. Metabolic adaptation of human pathogenic and related nonpathogenic bacteria to extra- and intracellular habitats. *FEMS Microbiol Rev* 36, 435–462, 2012.

- 12) Green P, Theilla M, Singer P. Lipid metabolism in critical illness. *Current Opinion in Clinical Nutrition and Metabolic Care* 19, 111–115, 2016.
- 13) Holmes E, Foxall PJ, Nicholson JK, Neild GH, Brown SM, Beddell CR, et al. Automatic data reduction and pattern recognition methods for analysis of <sup>1</sup>H nuclear magnetic resonance spectra of human urine from normal and pathological states. *Anal Biochem* 220, 284–296, 1994.
- 14) Ihaka R and Gentleman RR. A language for data analysis and graphics. *J Comput Stat Graph* 5, 299–314, 1996.
- 15) Larrouy-Maumus G. Lipids as biomarkers of cancer and bacterial infections. *Curr Med Chem* 26, 1924-32, 2019.
- 16) Meiboom S and Gill D. Modified spin-echo method for measuring nuclear relaxation times. *Rev Sci Instrum* 29, 688–691, 1958.
- 17) Mylonakis ME, Harrus S, Breitschwerdt EB. An update on the treatment of canine monocytic ehrlichiosis (*Ehrlichia canis*). *Vet J* 246, 45-53, 2019.
- 18) Neuhäuser M. Wilcoxon-Mann-Whitney Test. In: *International Encyclopedia of Statistical Science*, Lovric M. ed. Springer, Berlin, Heidelberg, pp. 1656-1658, 2011.
- 19) Sainz Á, Roura X, Miró G, Estrada-Peña A, Kohn B, Harrus S, et al. Guideline for veterinary practitioners on canine ehrlichiosis and anaplasmosis in Europe. *Parasit Vectors* 8,75, 2015.
- 20) Schwartz C, Katz DA, Larson M, Licciardi N, Kallick C, Timothy M, et al. The relationship between ehrlichiosis and the development of hematologic malignancies. *Medical Hypotheses* 121, 57–59, 2018.
- 21) Stringer KA, Serkova NJ, Karnovsky A, Guire K, Paine R, Standiford TJ. Metabolic consequences of sepsis-induced acute lung injury revealed by plasma <sup>1</sup>H-nuclear magnetic resonance quantitative metabolomics and computational analysis. *Am J Physiol Lung Cell Mol Physiol* 300, L4–L11, 2011.
- 22) Vignoli A, Ghini V, Meoni G, Licari C, Takis PG, Tenori L, et al. High-throughput metabolomics by 1D NMR. *Angew Chem Int Ed Engl*. doi:10.1002/anie.201804736, 2019.
- 23) Westerhuis JA, van Velzen EJ, Hoefsloot HC, Smilde AK. Multivariate paired data analysis: multilevel PLSDA versus OPLSDA. *Metabolomics* 6, 119–128, 2010.
- 24) Zhang A, Sun H, Yan G, Wang P. Metabolomics for biomarker discovery: Moving to the clinic. *BioMed Research International* 2015, 1-6, 2015.